A role for pericytes as microenvironmental regulators of human skin tissue regeneration

Sophie Paquet-Fifield,[1] Holger Schlüter,[1] Amy Li,[1,2] Tara Aitken,[2] Pradnya Gangatirkar,[1] Daniel Blashki,[1] Rachel Koelmeyer,[1] Normand Pouliot,[1] Manuela Palatsides,[1] Sarah Ellis,[1] Nathalie Brouard,[1] Andrew Zannettino,[2] Nick Saunders,[3] Natalie Thompson,[1] Jason Li,[1] and Pritinder Kaur[1,2]

[1]Research Division, Peter MacCallum Cancer Centre, St Andrew's Place, Melbourne, Victoria, Australia.
[2]Haematology Division, Institute of Medical and Veterinary Science, Adelaide, South Australia, Australia.
[3]Immunology and Metabolic Medicine, Diamantina Institute, University of Queensland, Princess Alexandra Hospital, Brisbane, Queensland, Australia.

The cellular and molecular microenvironment of epithelial stem and progenitor cells is poorly characterized despite well-documented roles in homeostatic tissue renewal, wound healing, and cancer progression. Here, we demonstrate that, in organotypic cocultures, dermal pericytes substantially enhanced the intrinsically low tissue-regenerative capacity of human epidermal cells that have committed to differentiate and that this enhancement was independent of angiogenesis. We used microarray analysis to identify genes expressed by human dermal pericytes that could potentially promote epidermal regeneration. Using this approach, we identified as a candidate the gene *LAMA5*, which encodes laminin α5, a subunit of the ECM component laminin-511/521 (LM-511/521). LAMA5 was of particular interest as we had previously shown that it promotes skin regeneration both in vitro and in vivo. Analysis using immunogold localization revealed that pericytes synthesized and secreted LAMA5 in human skin. Consistent with this observation, coculture with pericytes enhanced LM-511/521 deposition in the dermal-epidermal junction of organotypic cultures. We further showed that skin pericytes could also act as mesenchymal stem cells, exhibiting the capacity to differentiate into bone, fat, and cartilage lineages in vitro. This study suggests that pericytes represent a potent stem cell population in the skin that is capable of modifying the ECM microenvironment and promoting epidermal tissue renewal from non-stem cells, a previously unsuspected role for pericytes.

Introduction

It is well accepted that in addition to the intrinsic molecular regulators that control stem and progenitor proliferation and differentiation, the microenvironment or "niche" (1) is a critical extrinsic regulator of both tissue and stem cell self-renewal and homeostasis in diverse organisms (2). In higher organisms, it is evident that a complex molecular dialogue exists between the stem/progenitor compartment and the mesenchymal or stromal cells located adjacent to them. Certain features of the niche are highly conserved among species, e.g., secreted factors, cell-surface receptors, and ECM proteins. Not surprisingly, regulators of major biological properties including cell adhesion, proliferation, signaling, and differentiation are central to ordered stem cell and tissue renewal. Thus, a number of common molecular regulators have been identified in the microenvironment of diverse tissues (3, 4). Elegant studies in genetically engineered murine skin have shown that epidermal stem/progenitor self-renewal and differentiation, particularly to the hair follicle lineages, involve appropriate regulation of a myriad of interconnected pathways, involving the integrins, Wnt and Notch signaling; an array of molecular regulators, such as β-catenin, c-myc, Tcf/Lef, Gata-3, and Sox-9, in the stem cell compartment; and secreted proteins found in their localized microenvironment, including TGF-β, BMPs (reviewed in ref. 3), and laminin-511/521 (LM-511/521) (5). A critical role for molecular crosstalk between the epidermis and the underlying mesenchymal or dermal microenvironment has been well documented, and when inappropriately regulated, it can lead to impaired tissue repair and the development of cancer (6, 7). Despite the unequivocal existence of intercellular communication between the epidermis and dermis (8, 9), the specific cell types found within the microenvironment of these tissues that regulate epidermal renewal remain poorly understood.

In much of the published literature, cultured murine embryonic (Swiss 3T3 J2) or human skin fibroblasts have been used to represent the dermis in cocultures. For example, the dependency of epidermal cells on fibroblast feeder layers for extended culture is well recognized (10); and the inclusion of fibroblasts in a "dermal equivalent" in organotypic cultures (OCs) is essential to recapitulate the highly organized epidermal tissue architecture and temporal pattern of differentiation-specific gene expression. However, the precise relationship of fibroblasts to the stromal cell types found in the dermis in vivo remains unclear, although the inclusion of *endothelial* cells in the dermal equivalent of OCs dramatically enhances epidermal differentiation and basement membrane assembly (11). Interestingly, some epithelial cancers arise as a direct result of mutations in the mesenchymal cells (12), indicating the need to gain a better understanding of the role of various cell types found in the complex microenvironment of higher mammalian tissues.

In an attempt to define a possible role for new mesenchymal cell types in the niche of epithelial tissues, we raised mAbs against uncultured human skin dermal cells and identified mAb HD-1,

Authorship note: Sophie Paquet-Fifield and Holger Schlüter contributed equally to this work.

Conflict of interest: The authors have declared that no conflict of interest exists.

Citation for this article: *J. Clin. Invest.* **119**:2795–2806 (2009). doi:10.1172/JCI38535.

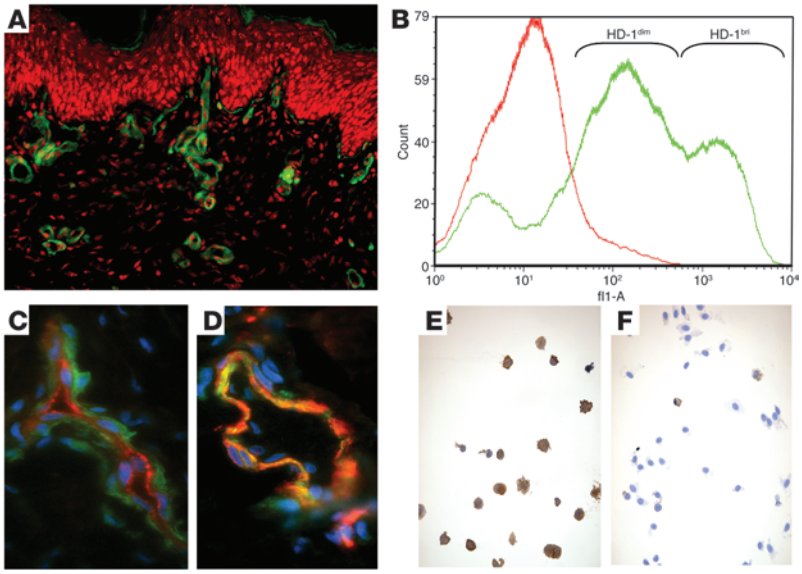

Figure 1
mAb HD-1 recognizes a subpopulation of pericyte-like dermal cells in close contact with the epithelium. (**A**) In situ immunostaining with mAb HD-1 on 3-μm-thick frozen sections of neonatal foreskin. HD-1–positive cells (green, FITC) were detected in the dermis underlying basal epithelial keratinocytes. Nuclei are stained red with propidium iodide. This image is representative of more than 50 independent samples. Original magnification, ×10. (**B**) Single color flow cytometric analysis of a typical human dermal cell suspension stained with mAb HD-1 (green line) or an isotype-matched control (IgG_1, red line), illustrating the presence of HD-1^{dim} and HD-1^{bri} fractions. A total of 10,000 7AAD-negative (i.e., living) cells were analyzed. (**C** and **D**) In situ immunostaining of frozen sections of human upper dermis costained with mAb HD-1 (green) and the endothelial marker vWF (red, **C**) illustrating that mAb HD-1 recognizes pericytes surrounding the vWF-positive endothelial cells lining the blood vessel. (**D**) Colocalization of the pericyte marker ACTA2, or SMA (red, **D**), and the HD-1 antigen (green). Nuclei are stained blue with DAPI. Original magnification, ×60. (**E** and **F**) Cytospins of the HD-1^{dim} and HD-1^{bri} fractions of human neonatal foreskin dermal cell isolates collected by FACS and stained for the pericyte marker ACTA2. The HD-1^{bri} cells (**E**) were positive for ACTA2, in contrast to the HD-1^{dim} cells (**F**). These pictures are representative of 3 independent sorting and staining experiments. Original magnification, ×20.

which recognizes pericytes located adjacent to the proliferative basal layer of the skin's epidermis. Here we report a previously unrecognized role for pericytes in promoting epithelial proliferation, differentiation, and tissue regeneration in the *absence* of angiogenesis, in contrast to their well-known ability to regulate endothelial cell function (13). Consistent with the reported ability of pericytes to act as mesenchymal stem cells (MSCs) in a variety of tissues (14), we demonstrate the capacity of the human dermal pericyte bulk population to differentiate into the bone, fat, and cartilage lineages. Further, we describe the molecular signature of dermal pericytes and show that these cells synthesize and secrete in situ the α5 chain of LM-511/521 — a protein previously shown by us to recruit differentiating epidermal cells to proliferate and reconstitute skin tissue (15). These results represent a paradigm shift in the current understanding of the role of dermal pericytes in homeostasis and disease throughout the body given their ubiquitous presence in all vascularized tissues. Our results further suggest that pericytes are important microenvironmental regulators of skin regeneration, an observation that could be exploited for ex vivo expansion of epidermal progenitors for the treatment of skin deficits.

Results

Identification of dermal pericytes in the microenvironment of human epidermal stem and progenitor cells, using a novel mAb, HD-1. Given the suitability of human skin as a model system for molecular crosstalk between epithelial tissues and their microenvironment and the paucity of tools to dissect stromal cells of human tissue, we generated novel mAbs against cell-surface markers expressed by freshly isolated primary dermal cells from neonatal human foreskin, with the aim of identifying functionally relevant subsets of cells in the immediate microenvironment, or niche, of epidermal stem and progenitor cells, using previously described methods (15, 16). The screening strategy (see Methods), led to the selection of a single mAb, human dermis–1 (HD-1), primarily because it recognized a discrete subset of dermal cells close to the epidermis (Figure 1A). Importantly, mAb HD-1 fractionated dermal cell isolates into 3 populations: (a) a relatively minor subset of 13% ± 1.4% (n = 7) expressing high levels of the antigen (termed HD-1^{bri} cells); (b) the majority of dermal cells expressing lower levels of this antigen (HD-1^{dim} cells); and (c) HD-1–negative cells (Figure 1B; n > 50; Supplemental Figure 1; supplemental material available online with this article; doi:10.1172/JCI38535DS1). Given the greater sensitivity of flow cytometric techniques compared with in situ immunofluorescence, we inferred that the HD-1^{bri} fraction represented the positive cells visualized by in situ staining, whereas the HD-1^{dim} cells appeared negative in situ (Figure 1B), consistent with their 10-fold-lower expression of this antigen (10^2 versus 10^3; Figure 1A). Given that staining with mAb HD-1 revealed a blood vessel–like distribution in the dermis (Figure 1A), we stained simultaneously for HD-1 antigen and vWF, known to be expressed by endothelial cells. Figure 1C shows that while vWF was indeed found in the inner cells lining the microvessels as expected, HD-1 reactivity was present in adjacent perivascular cells, suggesting that HD-1^{bri} cells could be pericytes. The best known marker for pericytes in vivo is ACTA2 (also known as SMA) (17); dual staining for this cytoskeletal protein and the HD-1 antigen on skin sections revealed their consistent colocalization, as shown in Figure 1D. Further, immunostaining cytospins of HD-1^{bri} and HD-1^{dim} populations collected by fluorescence-activated cell sorting (FACS) clearly demonstrated that the HD-1^{bri} fraction was ACTA2 positive (Figure 1E; n > 5), in contrast to the HD-1^{dim} population (Figure 1F).

The purity of the HD-1^{bri} fraction was further confirmed by dual flow cytometric analysis with mAb HD-1 against lineage-specific markers for a number of non-fibroblastic cell types known to exist in the dermis, i.e., $CD31^+$ endothelial cells, $CD68^+$ macrophages, $CD33^+$ myeloid cells, $CD45^+$ leukocytes and dendritic cells, and $HLA\text{-}DR^+$ antigen-presenting cells. Results shown in Supplemental Figure 1 demonstrate that minor subsets of cells expressing all these antigens (except CD31) were detected in the dermal isolates; notably, these populations cofractionated with the HD-1^{dim} or HD-1^- fractions, but not with the HD-1^{bri} cells.

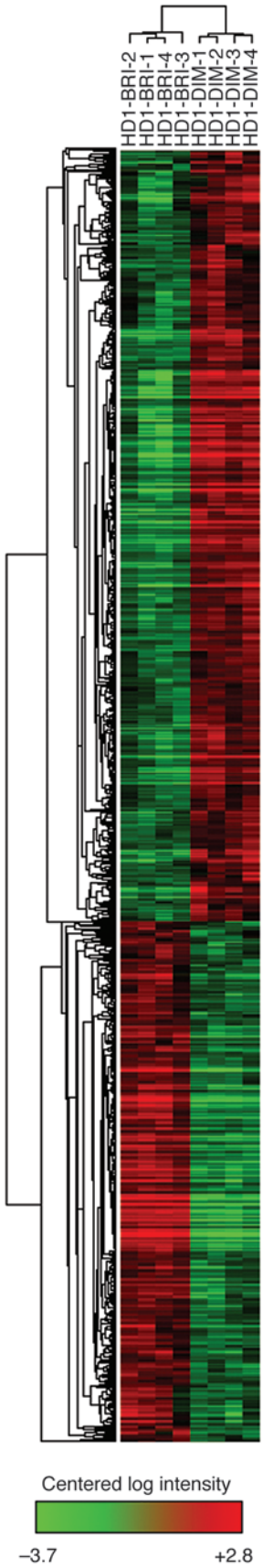

Figure 2
HD-1^{dim} cells and HD-1^{bri} cells display a distinct molecular profile. Microarray analyses of neonatal human dermal HD-1^{bri} and HD-1^{dim} populations from 4 independent FACS experiments, visualized using Treeview software, obtained by displaying a hierarchical cluster with average linkage analysis of normalized gene expression (>2-fold change, adjusted *P* values less than 0.05). These data illustrate the 2,288 probe sets differentially overexpressed (red) or underexpressed (green) in the HD-1^{bri} cells compared with the HD-1^{dim} population. The gene expression patterns are consistent among the 4 replicate experiments.

These phenotypic data were then confirmed using a global approach to determine the molecular signature of HD-1^{bri} cells using microarrays (Figure 2). Specifically, mRNA was obtained from the HD-1^{bri} and HD-1^{dim} populations by FACS from 4 independent sorts of neonatal human foreskin dermal cells and used to interrogate the human genome on Affymetrix Human Genome U133 Plus 2.0 arrays. These data reveal reproducible gene expression patterns observed among the 4 replicates (Figure 2); and the unique and distinct molecular signature of HD-1^{bri} and HD-1^{dim} populations. Notably, the identity of HD-1^{bri} cells as pericytes was confirmed by the differential expression of several known markers of pericytes, such as SMA, non-muscle myosin, tropomyosin 1 and 2, regulator of G protein signaling 5, chondroitin sulfate proteoglycan–4 (CSPG-4)/NG2, PDGFRB, aminopeptidase A and N, calponin, and caldesmon (Table 1). Consistent with the widely accepted role for pericytes in regulating endothelial cell function (18), we observed overexpression of genes from molecular pathways related to angiogenesis, including endothelin, integrin, and Notch signaling pathways (Supplemental Table 1). In contrast, the HD-1^{dim} population overexpressed genes classified under immune defense/activation, inflammation, and immunity, e.g., chemokines and complement activators. Signaling pathways exclusively represented in the HD-1^{dim} cells included the interleukin, IGF, and T and B cell activation pathways (data not shown), consistent with the flow cytometric data (Supplemental Figure 1), confirming cofractionation of leukocytes in the HD-1^{dim} fraction. Taken together, the perivascular location of HD-1^{bri} cells combined with their expression of SMA, immunophenotype, and molecular signature provide compelling evidence that mAb HD-1 is capable of enriching for pericytes of the human dermis — an important advance given that currently, multiple surface markers are required to purify these cells (14).

HD-1^{bri} pericytes are distinct from HD-1^{dim} dermal fibroblasts and are lost from standard dermal cell culture conditions. It is well recognized that pericytes have stringent growth requirements in culture (19), compared with fibroblasts. We therefore set out to test whether HD-1^{bri} pericytes were present in dermal cultures using two approaches. (a) Flow cytometric analysis of P7 human foreskin fibroblasts (HFFs; which are routinely maintained in DMEM plus 10% serum [DMEM-10]) revealed that the HD-1^{bri} pericyte population was no longer detectable when stained with mAb HD-1, although the HD-1^{dim} population persisted (Supplemental Figure 2A; $n = 5$). (b) FACS-purified HD-1^{bri} and HD-1^{dim} fractions were cultured in DMEM-10 and their growth assessed 14 days later. While the HD-1^{dim} cells gave rise to long-term cultures of fibroblastic cells (Supplemental Figure 2, B, bottom row, and D), the HD-1^{bri} pericyte population did not proliferate in this medium (Supplemental Figure 2B, top row), although we consistently observed initial attachment and spreading of these cells (Supple-

Table 1
Differential expression of selected genes overexpressed in the HD-1^{bri} dermal pericyte population

Gene symbol	Gene name	GenBank accession no.	log_2 fold	Adjusted *P* value
Cell-surface markers				
AOC3	Adhesion protein 1	NM_003734	4.43	2.85×10^{-8}
CDH6	Cadherin 6, type 2, K-cadherin	AU151483	4.39	2.12×10^{-9}
		BC000019	4.39	2.12×10^{-9}
		BF344237	2.54	1.46×10^{-7}
GJA4	Gap junction protein, alpha 4, 37kDa (connexin 37)	M96789	3.50	6.36×10^{-8}
		NM_00206	2.90	1.15×10^{-7}
ITGA7	Integrin, alpha 7	AF072132	4.17	3.07×10^{-8}
		AK022548	3.92	1.12×10^{-8}
JAG1	Jagged 1	U61276	2.76	6.76×10^{-8}
		U77914	2.14	1.11×10^{-7}
		AI457817	2.36	2.03×10^{-6}
		U73936	2.04	1.12×10^{-7}
MCAM (CD146)	Melanoma cell adhesion molecule	M29277	4.12	8.73×10^{-9}
		AF089868	3.69	904×10^{-9}
		BE964361	3.21	1.98×10^{-8}
		M28882	3.28	4.60×10^{-9}
NOTCH3	Notch homolog 3	NM_000435	3.54	1.36×10^{-8}
ITGA1	Integrin alpha 1, Pelota homolog	BG619261	3.40	1.48×10^{-7}
		X68742	2.63	6.91×10^{-5}
		NM_015946	1.61	8.96×10^{-7}
		AA156783	3.41	3.19×10^{-7}
Secreted factors				
A2M	Alpha-2-macroglobulin	NM_000014	1.82	1.97×10^{-6}
ANGPT2	Angiopoietin 2	NM_001147	3.03	1.11×10^{-5}
		AA083514	2.72	9.29×10^{-6}
		AF187858	2.46	8.50×10^{-6}
BMP2	Bone morphogenetic protein 2	NM_001200	1.26	1.19×10^{-5}
		AA583044	1.35	1.52×10^{-6}
CCL8	Chemokine (C-C motif) ligand 8	AI984980	3.82	2.56×10^{-7}
ECRG4	Esophageal cancer related gene 4 protein	AF325503	5.04	2.78×10^{-7}
FRZB	Frizzled-related protein	U91903	2.83	1.13×10^{-7}
		NM_001463	2.76	2.32×10^{-7}
PDGFA	Platelet-derived growth factor alpha polypeptide	NM_002607	3.59	2.18×10^{-7}
		AW205919	3.30	7.45×10^{-8}
		X03795	2.97	1.31×10^{-7}
ECM proteins				
ADAMTS5	ADAM metallopeptidase (aggrecanase-2)	AI123555	1.40	1.70×10^{-6}
		BF060767	1.40	3.01×10^{-6}
		NM_007038	1.28	5.07×10^{-6}
COL4A1	Collagen, type IV, alpha 1	NM_001845	2.35	3.41×10^{-6}
		AI922605	1.62	1.51×10^{-6}
COL4A2	Collagen, type IV, alpha 2	AA909035	2.13	1.61×10^{-6}
		X05610	1.66	1.67×10^{-6}
LAMA3	Laminin, alpha 3	NM_000227	3.03	4.58×10^{-8}
LAMA5	Laminin, alpha 5	BC003355	2.39	2.69×10^{-7}
NTN4	Netrin 4	AF278532	1.51	4.62×10^{-5}
TNC	Tenascin C	AI266750	2.20	2.58×10^{-6}
Pericyte markers				
ACTA2	Actin, smooth muscle aorta	AI917901	2.94	5.03×10^{-6}
		NM_001613	2.96	2.03×10^{-8}
MYH9	Myosin, heavy polypeptide 9, non-muscle	AI827941	1.23	3.69×10^{-6}
TPM1	Tropomyosin 1	NM_000366	2.73	1.11×10^{-7}
		NM_000366	1.70	4.75×10^{-6}
		Z24727	2.15	3.22×10^{-7}
		M19267	2.33	5.39×10^{-8}
TPM2	Tropomyosin 2	NM_003289		
RGS5	Regulator of G-protein signaling 5	AF493929	1.29	9.68×10^{-7}
		AI183997	5.83	1.52×10^{-8}
		AF159570	5.23	4.24×10^{-8}
		NM_025226	5.73	1.52×10^{-8}
CSPG4/NG2	Chondroitin sulfate proteoglycan 4	NM_001897	1.03	2.07×10^{-6}
		BE857703	1.75	3.50×10^{-6}
PDGFRB (CD140B)	Platelet-derived growth factor receptor	NM_002609	1.28	1.22×10^{-6}
ENPEP	Glutamyl aminopeptidase (aminopeptidase A)	L12468	2.77	9.17×10^{-6}
		NM_001977	2.83	2.39×10^{-6}
CNN1	Calponin 1, basic smooth muscle	NM_001299	2.34	3.41×10^{-7}
CALD1	Caldesmon 1	AI685060	1.89	1.44×10^{-5}
		AL577531	1.83	2.95×10^{-7}
		NM_004342	2.20	3.44×10^{-7}
		AL583520	1.04	7.15×10^{-6}

The table summarizes selected groups of genes that had a log_2 fold expression greater than 2 and *P* value less than 0.05 in the HD-1^{bri} population, chosen for their biological relevance, i.e., cell-surface markers, secreted factors, ECM proteins, and pericyte markers. The pericyte nature of the HD-1^{bri} cells was confirmed by the differential expression of a large number of reported pericyte-associated genes, including *ACTA2* (also known as SMA), *NG2*, *RGS5*, *PDGFRB*, aminopeptidase A and N, calponin, and caldesmon.

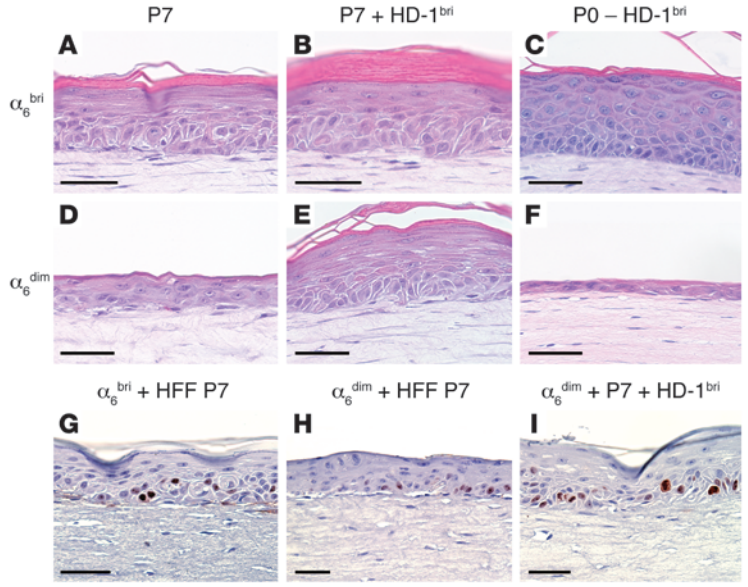

Figure 3
The inclusion of HD-1^{bri} pericytes in the dermal equivalent of OCs reconstituted with P7 HFFs stimulates epidermal regeneration capacity of α_6^{dim} differentiating keratinocytes. Sections of OCs stained with H&E showing reconstituted skin tissue from α_6^{bri} (stem and TA) keratinocytes (**A**–**C**) or α_6^{dim} early differentiating keratinocytes (**D**–**F**) grown on dermal equivalents containing either P7 HFFs alone (**A** and **D**), P7 HFFs plus 10% HD-1^{bri} cells (**B** and **E**), or fresh HFFs depleted of HD-1^{bri} cells (**C** and **F**). The intrinsically low epidermal tissue-regenerative capacity of α_6^{dim} keratinocytes is substantially enhanced by coculture with dermal equivalents containing HD-1^{bri} cells (**E**; $n = 3$), while depletion of HD-1^{bri} cells diminishes their tissue-regenerative capacity (**F**; $n = 2$). Notably, the α_6^{bri} stem and TA–containing fraction exhibits excellent tissue regeneration irrespective of the presence of pericytes (**A**–**C**; $n = 3$). (**G**–**I**) Ki67 staining of OCs of α_6^{bri} (stem and TA) keratinocytes (**G**) or α_6^{dim} early differentiating keratinocytes (**H** and **I**) grown on dermal equivalents containing either P7 HFFs alone (**G** and **H**) or P7 HFFs plus 10% HD-1^{bri} cells (**I**). Note the increase in cellularity and number of Ki67-positive cells in the α_6^{dim} epithelium upon coculture with the HD-1^{bri} cells compared with P7 HFFs alone (**I** versus **H**), restoring epithelial regeneration to levels comparable to those obtained with the α_6^{bri} stem and TA compartment (**G**). Scale bars: 100 μm.

mental Figure 2E; $n > 10$). Notably, the HD-1^{bri} pericytes (and the HD-1^{dim} cells) could be expanded in α-MEM medium supplemented with 20% serum and 1 ng/ml PDGF (Supplemental Figure 2C; $n = 4$), displaying pericyte-like morphology, i.e., large, irregular cells (19) evident at low density (see Supplemental Figure 2F). These data demonstrate that the HD-1^{dim} fraction enriches for the fibroblast population (HFFs), which is easily propagated in various culture conditions, whereas the HD-1^{bri} pericyte population requires more selective conditions.

Pericytes promote the tissue-regenerative ability of differentiating keratinocytes in the absence of angiogenesis. We have previously shown that the growth and tissue-regenerative capacity of epidermal stem cells and their progeny can be significantly modulated by their dermal cellular and molecular microenvironment. Notably, primary human keratinocytes that have initiated differentiation, with the cell-surface phenotype integrin α_6^{dim} — as determined by numerous criteria reported by us previously (e.g., expression of epidermal differentiation markers K10 and involucrin; poor short- and long-term proliferative output in vitro; refs. 16, 20) — exhibited limited growth and tissue-regenerative ability in OCs, when cocultured with P7 HFFs (Figure 3D), compared with the keratinocyte stem cell (KSC; $\alpha_6^{bri}CD71^{dim}$) and transit amplifying (TA; $\alpha_6^{bri}CD71^{bri}$) compartment of the epidermis, either alone (15) or when combined (i.e., α_6^{bri} proliferative compartment; Figure 3A). Specifically, the α_6^{dim}-derived epithelium exhibited markedly lower cellularity in the basal layer, disorganized suprabasal layers, fewer layers in the stratum corneum, and an irregular distribution of Ki67-positive cells (Figure 3, D and H) compared with the α_6^{bri}-derived epithelium (Figure 3, A and G). However, substitution of the passage 7 (P7) HFFs for minimally passaged HFFs (i.e., P0–P2) in the OCs resulted in impressive tissue-regenerative ability from the α_6^{dim} differentiating keratinocytes, essentially indistinguishable from that of the stem cell and TA fractions (15). These observations and the more stringent growth requirements of pericytes (Supplemental Figure 2) led us to speculate that the loss of pericytes may potentially account for the decreased tissue-regenerative capacity of committed keratinocytes. In order to test our hypothesis, firstly, we collected HD-1^{bri} dermal foreskin pericytes by FACS and coinoculated them at an incidence of 10%–50% of P7 HFFs into the dermal equivalents of OCs, prior to plating the α_6^{dim} epidermal cells on top. α_6^{bri} epidermal cells (i.e., the combined stem and TA keratinocytes) were used as positive controls. Results obtained from 3 independent sorting experiments showed that the poor tissue-regenerative capacity of α_6^{dim} keratinocytes compared with the α_6^{bri} keratinocytes cocultured with P7 HFFs (Figure 3, A and D) could be significantly enhanced by the inclusion of HD-1^{bri} pericytes in the OCs (Figure 3E; $n = 3$). Indeed, the HD-1^{bri} cells could induce the previously differentiating α_6^{dim} keratinocytes to regenerate an epithelium morphologically similar to that obtained from the combined keratinocyte stem and TA populations (Figure 3, E versus B), with respect to increase in cellularity throughout the epithelium and distribution of Ki67-positive cells (Figure 3, I versus H). The dependency of the α_6^{dim} keratinocytes on pericytes was further illustrated by a second experimental approach, whereby HD-1^{bri} cells were depleted from isolates of primary dermal cells by FACS and the remaining dermal cells used to reconstitute the dermal equivalents. The results shown in Figure 3F ($n = 2$) demonstrate that the α_6^{dim} keratinocytes were unable to regenerate an extensive epithelium in the absence of pericytes, although the combined stem and TA compartment (α_6^{bri}) proceeded to proliferate and differentiate normally under these conditions (Figure 3C; $n = 2$). These data clearly demonstrate that while the proliferative cells of the epidermis possess great intrinsic tissue-regenerative capacity, cells that have committed to differentiate can be induced to resume proliferation and reform epidermal tissue in response to their microenvironment, presumably due to secreted factors produced by the HD-1^{bri} pericytes of the dermis. Notably, in the OC model, blood vessel formation does not take place. Thus, while one might expect pericytes to improve wound healing indirectly through promoting angiogenesis in vivo, here we report a role for pericytes in supporting the proliferation of epithelial cells in its absence — an observation that has profound implications for proliferative disorders of epithelial tissues including cancer, given the widespread distribution of pericytes throughout the body.

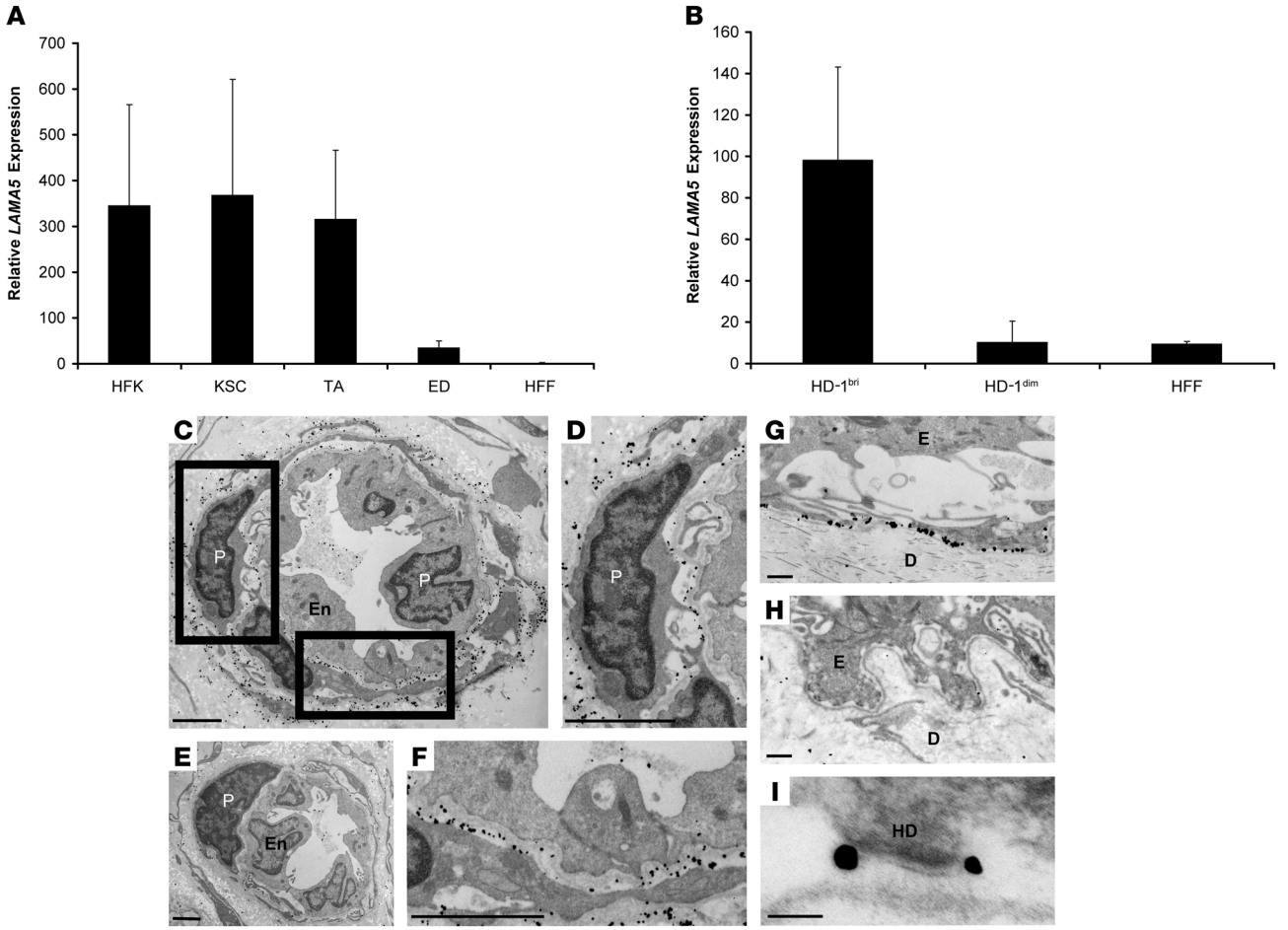

Figure 4

Human dermal pericytes synthesize and secrete LAMA5 in the skin. (**A**) Quantification of *LAMA5* mRNA expression by RT-PCR in freshly sorted epidermal cell populations from human neonatal foreskin. *LAMA5* mRNA was highly expressed in unfractionated human foreskin keratinocytes (HFK), KSCs, and TA keratinocytes; and downregulated in early differentiating keratinocytes (ED). *LAMA5* was undetectable in HFFs. (**B**) *LAMA5* mRNA expression by RT-PCR in HD-1^{bri} cells, HD-1^{dim} cells, and HFFs, illustrating overexpression in the HD-1^{bri} pericytes. In **A** and **B**, data represent results from 3 independent sorting experiments; mean ± SEM is shown. (**C**–**I**) Immunogold electron microscopic localization of human LAMA5 with mAb 4C7 in skin sections. LAMA5 was detected in the basement membrane between the endothelial cells (En) of blood vessels and the surrounding pericytes (P) (**C** and **F**); in the basement membrane region between the epidermis (E) and dermis (D) (**G**); and at hemidesmosomes (HD) (**I**). In addition, immunogold particles were also localized abluminally, i.e., secreted into the dermal space at the periphery of pericytes (**D**). Labeling with isotype-matched negative control mAb 1D4.5 showed the absence of staining in skin sections, as shown for blood vessels (**E**) and the epidermal-dermal junction (**H**). (**D** and **F**) Higher-magnification views of regions indicated in **C**. Scale bars in **C**–**F**: 10 μm; **G** and **H**: 0.5 μm; **I**: 0.1 μm.

Dermal pericytes synthesize and secrete LM-511/521, a basement membrane ECM protein known to promote epidermal tissue regeneration from α_6^{dim} differentiating keratinocytes. In an attempt to understand how HD-1^{bri} cells could promote epidermal regeneration, we scanned our microarray data for secreted growth factors and ECM proteins known to promote epithelial growth, particularly FGF-7/keratinocyte growth factor (FGF-7/KGF) and FGF-10, which act via a common receptor (21–23). Differential expression of FGF-7 and -10 was not detected by microarray in either the HD-1^{bri} or HD-1^{dim} fractions. IL-1 has been reported to be secreted by keratinocytes under perturbed conditions (24), which promotes FGF-7 production in dermal fibroblasts (25, 26). Interestingly, the IL-1 receptor types 1 and 2 were expressed by the HD-1^{dim} fraction and not the HD-1^{bri} pericytes ($P = 3.98 \times 10^{-6}$ and $P = 9.85 \times 10^{-5}$, respectively), suggesting that it is the HD-1^{dim} cells rather than the pericytes that are poised to respond to an IL-1 stimulus upon wound healing.

We have previously reported that an exogenous supply of LM-511/521 can increase the proliferative ability of α_6^{dim} keratinocytes in culture and improve their intrinsically poor tissue-regenerative capacity in OCs with P7 HFFs in the dermal equivalent (15). The synthesis and deposition of the rate-limiting LAMA5 chain of these laminin isoforms is normally attributed to epidermal keratinocytes, given its localization on the epithelial side of the basement membrane, although studies indicate that molecular crosstalk between epithelial and mesenchymal cells promotes its synthesis and deposition (27). The microarray data showed that this ECM protein was consistently overexpressed by the HD-1^{bri} pericytes

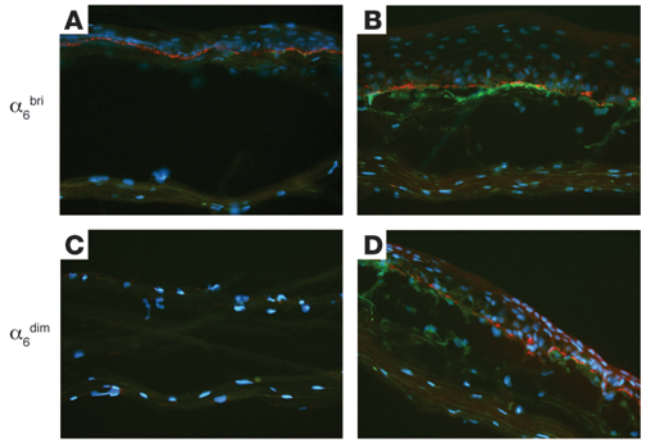

Figure 5
Increased deposition of LAMA5 by α_6^{dim} keratinocytes cocultured with HD-1^{bri} pericytes in OCs. Immunofluorescence staining for LAMA5 (mAb 4C7, red) and HD-1 antigen (green) performed on 3-μm frozen sections of OCs, showing epithelial sheets regenerated by α_6^{bri} (combined stem and TA; **A** and **B**) or α_6^{dim} early differentiating keratinocytes (**C** and **D**) seeded on a dermal equivalent containing either P7 HFFs alone (**A** and **C**) or P7 HFFs plus HD-1^{bri} pericytes (**B** and **D**). Nuclei were counterstained with DAPI (blue). LAMA5 immunostaining in the epidermal-dermal junction was observed in all OCs reconstituted with α_6^{bri} keratinocytes, irrespective of the presence of pericytes (**A** and **B**). In contrast, OCs reconstituted with α_6^{dim} keratinocytes cocultured with HD-1^{bri} pericytes (**D**) displayed largely increased LAMA5 levels compared with controls (**C**). HD-1 staining revealed the localization of pericytes in close proximity to the epidermal cells in OCs, where they were added back to the dermal equivalents (**B** and **D**). Original magnification, ×20.

(Table 1) at a 7-fold-higher level compared with the HD-1^{dim} fraction of the dermis in all 4 replicate experiments. Further, real-time RT-PCR analysis confirmed the preferential expression of the α5 chain of LM-511/521 in the pericyte population compared with the HD-1^{dim} cells (Figure 4B). Similar analysis among epidermal keratinocytes fractionated into α_6^{bri}CD71^{dim} stem, α_6^{bri}CD71^{bri} TA, and α_6^{dim} early differentiating compartments revealed that the proliferative cells (stem and TA) contained more transcripts for the α5 chain of LM-511/521 than the differentiating α_6^{dim} cells (Figure 4A) — an observation consistent with the latter cells preparing to detach from the basement membrane in vivo as they start differentiating.

In order to determine whether the LAMA5 mRNA was translated into protein in vivo, we performed immunogold staining for electron microscopy on neonatal human foreskin sections. Our results confirmed the localization of this protein in the basement membrane: (a) directly below epidermal keratinocytes (Figure 4G) at the dermal-epidermal junction; close to hemidesmosomes (Figure 4I); and (b) at the pericyte–endothelial cell junction of microvessels in the skin (Figure 4, C and F). To our surprise, immunogold particles could also be seen in the perivascular space on the abluminal side of the blood vessels, indicating the secretion of the α5 chain of LM-511/521 into the dermal space (Figure 4, C and D). These data show for the first time to our knowledge that cells present in the immediate microenvironment of epidermal cells are capable of synthesizing a protein that has profound effects on promoting epithelial cell and tissue regeneration (15, 28). We therefore asked whether the introduction of pericytes into OCs could act to compensate the intrinsically low levels of LM-511/521 produced by the α_6^{dim} keratinocytes, thereby promoting tissue regeneration. Immunostaining of the OCs of α_6^{dim} cells in which HD-1^{bri} pericytes had been reintroduced revealed an increase in the detectable levels of the α5 chain of LM-511/521 in the dermal-epidermal junction (Figure 5D) compared with controls (Figure 5C), although its distribution was uneven. Consistent with the RT-PCR data (Figure 4A), the LAMA5 chain was detected in OCs derived from the combined stem and TA fractions, irrespective of the presence of pericytes. Immunostaining of the OCs with mAb HD-1 (Figure 5, A–D) revealed the presence of pericytes in the dermal equivalent of those cocultures that had been inoculated with them (Figure 5, B and D), demonstrating that the pericytes persist in the OCs. Notably, the HD-1^{bri} cells were found in close apposition to the epidermal cells compared with fibroblasts that were distributed throughout the dermal equivalent of the OCs. This suggests that the pericytes migrate to the dermal-epidermal junction in vitro, despite the lack of blood vessels, and form an important microenvironmental element of epithelial tissues. This idea is consistent with the recent report by Crisan et al. (14) that cultured perivascular cells migrate toward sites of tissue injury characterized by degraded ECM. Interestingly, mAb HD-1 stained perivascular SMA and NG-2/CSPG-4–positive cells surrounding blood vessels in adult human skin (Supplemental Figure 3), as observed in neonatal foreskin. Interestingly, expression of NG-2/CSPG-4, also known as melanoma chondroitin sulfate proteoglycan (MCSP), was not restricted to the dermis and was detectable in both adult and neonatal keratinocytes (Supplemental Figure 3, B and F) as reported previously (29). mAb HD-1 also stained pericytes in many other tissues, i.e., human adult aorta, kidney, brain, pancreas, thymus, and lung (data not shown), demonstrating its versatility in identifying pericytes outside skin.

Human dermal pericytes exhibit functional and phenotypic properties of MSCs. It has recently been suggested that pericytes at a number of locations in the human body are MSCs and as such are capable of differentiating into multiple lineages. We therefore tested whether the HD-1^{bri} pericytes of human skin could differentiate into the fat, bone, and cartilage lineages by placing this bulk population of cells into the appropriate inductive culture conditions. The results of a representative experiment are shown in Supplemental Figure 4 and were replicated at least 3 times. Adipogenic culture medium induced the accumulation of oil red O–positive lipid droplets within the pericytes but not in controls (Supplemental Figure 4, A and B). Similarly, deposition of calcium triphosphate mineral stained brown with von Kossa reagent was observed in HD-1^{bri} pericyte cultures under osteogenic culture conditions compared with controls, demonstrating differentiation into the bone lineage (Supplemental Figure 4, C and D). Finally, the dermal HD-1^{bri} pericytes when subjected to micromass culture showed evidence of chondrocyte differentiation both morphologically and when stained for proteoglycans with Alcian blue (Supplemental Figure 4, E and F). These results confirmed that dermal skin pericytes had the capacity for differentiation into various mesenchymal cell lineages, as reported for pericytes from other body sites (14), although the extent to which all HD-1^{bri} cells could do this homogeneously was not investigated in this study.

Given these functional MSC-like properties of the human skin HD-1^{bri} pericyte population, we sought to determine whether the latter cells expressed known MSC markers, particularly

CD73, CD90/Thy-1, CD146/MCAM, and CD105/endoglin (14), using flow cytometry. These data revealed that the HD-1^{bri} population expressed all but one MSC marker analyzed and were CD146$^+$CD73$^+$CD90$^+$ (Supplemental Figure 5; $n = 3$). Interestingly, the expression of CD146, CD73, and CD90 was not exclusive to the HD-1^{bri} population but was also found on the HD-1^{dim} fibroblast population, albeit at different levels. Thus, CD146 was expressed at higher levels (Supplemental Figure 5, D and H), while CD73 was only weakly expressed on the HD-1^{bri} pericytes (Supplemental Figure 5, A and E) compared with the HD-1^{dim} population. CD90 was expressed widely in the dermis, including HD-1^{bri} pericytes, HD-1^{dim} fibroblasts, and CD45$^+$ cells (Supplemental Figure 5, B and F). Notably, CD105, a well-characterized marker for bone marrow–derived and other MSCs and large-vessel endothelial cells, was not expressed by the HD-1^{bri} cells, although a subset of HD-1^{dim}CD45$^+$ cells of the dermis were positive for CD105 (Supplemental Figure 5, C and G), with light scatter characteristics of white blood cells (data not shown). Thus, although considerable overlap in function and phenotype was observed between MSC populations reported in the literature and HD-1^{bri} pericytes, MSC markers were also found on HD-1^{dim} fibroblasts and CD45$^+$ dermal cells.

mAb HD-1 recognizes the $\alpha_1\beta_1$ integrin. In order to determine the identity of the epitope recognized by mAb HD-1, we used cultured fibroblasts that also expressed this epitope (Figure 1B) to immunoprecipitate the antigen, since these cells could be expanded in sufficient quantities for these experiments. The multiple bands obtained in IPs combined with a distribution study among various cell types suggested to us that mAb HD-1 recognized $\alpha_1\beta_1$ integrin not expressed by epithelial cells (data not shown). We hypothesized that mAb HD-1 may recognize the collagen receptor $\alpha_1\beta_1$. We therefore immunoprecipitated the HD-1 antigen and the $\alpha_1\beta_1$ integrin with a known mAb to this cell adhesion molecule, i.e., mAb TS2/7.1.1 (HB-245; ATCC), from fibroblasts and blotted the IPs obtained with a blotting mAb against $\alpha_1\beta_1$, i.e., mAb 1973 (clone FB12; Chemicon), running commercially available purified $\alpha_1\beta_1$ protein (CC1015; Chemicon) as a positive control alongside the IPs (Supplemental Figure 6). The results obtained reveal that the α_1 blotting antibody detected two specific bands in the HD-1 and TS2/7.1.1 immunoprecipitates (lanes 1 and 3, compared with control precleared samples, lanes 2 and 4) and in the purified α_1 protein–positive control isolated from smooth muscle cells (lanes 7 and 8). The α_1 chain of the purified $\alpha_1\beta_1$ integrin has been reported at 195 kDa under reducing conditions in smooth muscle cells, which correlates with the lower band (30); the second, higher-molecular-weight band of approximately 205 kDa most likely represents the pro-α form of the integrin destined for endoproteolytic cleavage or a glycosylated version of the α_1 chain, given that these posttranslational modifications are widely reported for integrins (31, 32). The extra bands of low molecular weight observed in lanes 7 and 8 containing the purified protein are presumably degraded fragments of the α_1 protein. The additional low-molecular-weight bands observed in the IP lanes are immunoglobulin chains (of the mAbs used for IP), detected by the secondary antibody used for blotting, as shown by their presence in lanes containing the mAb HD-1 alone (lane 5) or mAb TS2/7.1.1 alone (lane 6). Further confirmation that mAb HD-1 detected α_1 integrin was provided by experiments in which preincubation of fibroblasts with mAb HD-1 blocked subsequent binding of mAb TS2/7.1.1 (compared with an isotype-matched control mAb), such that α_1 was no longer detectable by flow cytometry (data not shown). Consistent with this conclusion, the microarray data showed overexpression of α_1 in the HD-1^{bri} pericytes (Table 1, *ITGA1*) at statistically significant levels.

Discussion

Pericytes have been studied extensively in the context of endothelial cell function and are well known to not only stabilize blood vessel structure but also regulate endothelial proliferation and differentiation, microvascular perfusion, and permeability through paracrine regulators, e.g., TGF-β and vasoactive agents (reviewed in refs. 17, 18). Although pericytes share many properties with smooth muscle cells, particularly as contractile cells surrounding blood vessels that express ACTA2 (SMA), they can be distinguished by the fact that they occupy a specific niche physically juxtaposed to endothelial cells in microvessels. It has been recognized that targeting both endothelial cells and pericytes improves the efficacy of anticancer therapies by disrupting angiogenesis (33), presumably by destabilizing tumor vascularization. The recent discovery that pericytes in a wide range of human tissues can differentiate into multiple mesenchymal lineages (14) has led to the suggestion that these cells may also be capable of acting as MSCs in all tissues (34). Our data suggest additional biological properties for pericytes in regulating epithelial proliferation and tissue regeneration, adding to the repertoire of this increasingly interesting cell type found in most body tissues.

Informed by previous studies from our laboratory showing that epithelial tissue regeneration of skin epidermal stem and progenitors could be regulated by both intrinsic properties of the epithelial cells and extrinsic dermal regulators (15), we sought to identify functional elements of the dermis or microenvironment of keratinocytes. Utilizing an approach we had successfully employed in fractionating epithelial stem and progenitors previously (16), we raised antibodies against uncultured dermal cell isolates from human neonatal skin, selecting those that recognized cell-surface molecules, and detected cells that were close to the epidermis and therefore more likely to influence its proliferation and differentiation. mAb HD-1 satisfied these criteria, permitting the visualization of target cells both in situ and in dissociated dermal cell preparations. A number of approaches confirmed that the cells recognized by the mAb were pericytes, including their perivascular location in microvessels; coexpression of SMA, a well-known marker for pericytes (Figure 1); an absence of various lineage markers for other dermal cell types (including endothelial, leukocyte, hematopoietic, and dendritic cells; Supplemental Figure 1); their more fastidious growth requirements compared with fibroblasts (Supplemental Figure 2); and their molecular profile, featuring reported markers of pericytes including ACTA2/SMA, NG2/CSPG-4, RGS5 MCAM/CD146, and PDGFRB (Table 1). These microarray data represent what we believe to be the first complete molecular signature reported for human pericytes and also reveal a number of new cell-surface markers (cadherin-6, gap junction protein α4, and the integrins α_7 and α_1) preferentially expressed by these cells that can be used to further characterize the biological properties of these cells. The identification of integrin α_1 on pericytes was consistent with our finding that mAb HD-1 detects this cell adhesion molecule, as revealed by immunoprecipitation with mAb HD-1 and subsequent blotting with a known anti–α_1 integrin antibody (Supplemental Figure 6). This observation is also consistent with reports of α_1 integrin expression on smooth muscle cells (30). Although fibroblasts also express this integrin, the levels of expres-

sion were a log lower (Figure 1B). Similarly, other dermal cells of various lineages also expressed much lower levels of α_1 integrin, permitting enrichment of viable pericytes in the α_1 integrin bright peak (Supplemental Figure 1).

Having established a method for viably isolating dermal pericytes, we were able to test these cells functionally in OCs. Tissue reconstitution studies could therefore be performed by adding back or depleting pericytes from the dermal equivalents in order to determine the effects of gain and loss of dermal pericyte function. Although the stem and TA compartments exhibited significant tissue-reforming capacity irrespective of the presence of pericytes in coculture, these studies clearly illustrated the dependency of early differentiating/committed epidermal progenitors (α_6^{dim} cells) for tissue reconstitution (Figure 3E). A number of converging observations led us to speculate that this biological effect on the latter cells could be attributed at least in part to the increased deposition of LM-511/521. First, the microarray data showed that a number of ECM proteins were highly expressed in pericytes compared with fibroblasts, including the LAMA3 chains found in LM-332, LM-311, LM-321; and LAMA5 found in LM-511 and LM521. Second, our previous work had shown that the LAMA3 chain was deposited at the dermal-epidermal junction of OCs irrespective of their skin regenerative capacity (and thus unlikely to be functionally relevant), whereas LAMA5 was only found in those cultures that had good epidermal tissue regeneration (15). Further, the addition of exogenous LM-511/521 was capable of restoring the limited tissue reconstitution of α_6^{dim} differentiating cells in OCs (15). The secretion of the LAMA5 chain is considered to be a function of keratinocytes and a rate-limiting step for LM-511 and -521 assembly and deposition. Although this was confirmed by RT-PCR and immunogold electron microscopy staining for LAMA5 protein (Figure 4, A and G), we discovered that the HD-1^{bri} dermal pericytes also contained abundant transcripts for LAMA5 and that they secrete this protein into the dermal space in skin (in addition to depositing it in basement membranes adjacent to endothelial cells; see Figure 4). Consistent with this observation, OCs of α_6^{dim} cells into which pericytes had been reintroduced revealed abundant deposition of LAMA5 compared with controls (Figure 5, C and D). We infer from these studies that pericytes compensate for the inherently decreased levels of LAMA5 synthesized by differentiating keratinocytes, as illustrated by RT-PCR analysis (Figure 4A), and thereby promote epidermal regeneration, an observation that can be exploited for ex vivo expansion of epidermal progenitors for clinical application in skin deficits. This effect is most likely achieved by promoting epidermal proliferation, as demonstrated by us previously when plating neonatal α_6^{dim} (and also α_6^{bri} keratinocytes) on purified LM-511/521 in monolayer cultures (15). This proproliferative effect of exogenous LM-511/521 was even greater on adult human skin keratinocytes (6- to 7-fold) compared with neonatal keratinocytes (2-fold), as shown by us previously (35). It is also likely that LAMA5 may act in concert with or cooperate with secreted factors produced by pericytes, although we were unable to find any evidence in favor of well-known paracrine regulators such as KGF and GM-CSF. It is accepted that IL-1 is secreted by epithelial cells when perturbed, stimulating the production of KGF/FGF-7 and GM-CSF by dermal cells, both of which are capable of stimulating epidermal proliferation (25, 26). The receptors for IL-1 were expressed by the HD-1^{dim} fibroblasts, as revealed by microarray analysis, suggesting that this particular paracrine loop is not mediated by pericytes. A more global functional analysis of candidate growth factors secreted by pericytes that promote epithelial proliferation will form the basis of future investigations.

The demonstration that the HD-1^{bri} dermal pericyte population exhibits the capacity to differentiate into a number of mesenchymal lineages, i.e., fat, bone, and cartilage (Supplemental Figure 4), confirms and extends recent reports suggesting that pericytes from a number of body sites may be MSCs (14, 34). Indeed, the close phenotypic identity and multilineage potential of human dermal HD-1^{bri} pericytes to bone marrow MSCs, i.e., $CD45^-CD31^-SMA^+NG\text{-}2^+PDGFRB^+CD146^+CD73^+CD90^+$, located in a perivascular niche reported here confirms the identification of a previously unrecognized resident MSC population in skin. We found that the MSC marker CD105 was not expressed by dermal HD-1^{bri} pericytes (or indeed HD-1^{dim} dermal cells), although a minor subset of $CD45^+CD105^+$ cells was detectable in skin. Consistent with this, previous reports of CD105 expression in human and murine skin in situ demonstrate expression in keratinocytes, activated endothelial cells only, and activated macrophages and monocytes (36) but not in stromal cells of the dermis. (37, 38). Although CD105 has been reported to be expressed by fibroblastic skin-derived dermal cells, many of these studies were performed on long-term-cultured cells (reviewed in ref. 39), which could result in activation of CD105 expression. Since CD105 is stably expressed by MSCs in other tissues and upon subsequent culture (14), we conclude that its absence on dermal HD-1^{bri} pericytes is a distinguishing feature, excluding the possibility that they are circulating MSCs derived from other tissues.

Another population of MSC-like cells originating from skin, known as skin-derived precursors (SKPs), has already been described in murine skin and localized in the dermal papilla of hair follicles (40). Human foreskin–derived SKPs have also been reported and their ability to give rise to mainly neural lineages and smooth muscle cells in culture described (41). Since the location of human foreskin SKPs remains to be elucidated, and their phenotype and function has been described after propagation in sphere cultures, their relationship to the HD-1^{bri} cells is difficult to establish. The location of SKPs in the murine dermal papilla of the hair follicle suggests that they are analogous or identical to the multipotent hair follicle–associated dermal papilla or dermal sheath MSC-like cells described by Jahoda et al. (42). Although further work is required to establish the cell-surface phenotype for SKPs and the hair follicle–associated dermal stem cells, the distinct perivascular niche occupied by the HD-1^{bri} human dermal pericytes and the absence of hair follicles in neonatal foreskin suggest they are quite distinct from these previously described skin MSC populations. Given the accessibility and abundance of skin, dermal pericytes are a potentially abundant source of MSCs for therapeutic purposes in repairing tissues of mesenchymal origins.

In conclusion, we demonstrate an angiogenesis-independent role for pericytes in promoting epithelial cell proliferation and skin regeneration, notably from non-stem cells, by modifying their immediate ECM microenvironment. This previously unsuspected function for pericytes represents a paradigm shift in our understanding of the potential function of these cells and how they could be manipulated to improve ex vivo cell expansion for cells of epithelial origin. Given the distribution of these cells throughout the body, it is possible that they may be widely implicated in tissue repair and important extrinsic regulators of cell-regenerative activity. This study also has significant implications for our current understanding of the microenvironment of stem cells and their progeny during homeostasis, tissue repair, and cancer.

Methods

Generation of the HD-1 mAb. The use of mice for making mAbs was approved by the Institute of Medical and Veterinary Science Animal Ethics Committee, Adelaide. BALB/c mice were immunized twice by injection of the foot pad with 6×10^6 primary dermal cells. Antibody-producing cells isolated from the popliteal lymph nodes were fused with the NS1 myeloma cell line and hybridomas generated. Thirty-nine hybridoma supernatants were selected from the entire fusion for further characterization based on microscopic analysis of in situ staining of unfractionated primary dermal cells in 96-well plates, since their pattern of expression indicated the detection of cell-surface antigens. These hybridomas were then screened for staining in frozen sections of neonatal human foreskin, the major criteria for further selection being exclusive reactivity against subsets of dermal cells. This strategy allowed us to *exclude* those supernatants that showed reactivity against (a) both epidermal and dermal compartments; (b) all dermal cells; or (c) cells in the deep dermis that may not reasonably be expected to influence epithelial cell behavior. Three hybridomas were selected and cloned several times, and their reactivity with skin tissue reanalyzed, leading us to identify a single hybridoma (named mAb HD-1) that detected dermal cells close to the epidermis.

Isolation and flow cytometric analysis of primary basal keratinocytes and dermal cells. Neonatal foreskin tissue normally discarded after routine circumcision was collected after written, informed consent was obtained from guardians. All experimentation on human tissue was approved by the Peter MacCallum Cancer Centre Human Research Ethics Committee (project 03/44) in accordance with Institute policy 54.5, "Use of Human Tissue in Research."

Primary basal keratinocytes were isolated from human neonatal circumcised foreskins as described previously (16, 43). Staining and FACS of keratinocyte fractions was performed as described previously (16). Dermal cells were stained with mAb HD-1 (6 μg/ml), resuspended in 7-AAD, and sorted on a BD FACS Vantage DIVA. The collected fractions were routinely reanalyzed to confirm sort purity. All flow data were analyzed using FCS Express software (De Novo Software).

Immunostaining. Human neonatal foreskin was fixed for 20 minutes with 2% buffered formalin. Cryosections were blocked in PBS/0.05% Tween-20/2% goat serum and incubated with mAbs at room temperature for 1 hour (15). Cytospins of sorted cells were washed, collected in FCS, and centrifuged at 450 *g* for 5 minutes on SuperFrost Plus poly-L-lysine–coated slides (Menzel-Gläser, Thermo Scientific). Cytospins were dried overnight or frozen at –80°C and processed for SMA staining after inactivation of endogenous peroxidase (3% H_2O_2, 10 minutes at room temperature).

Keratinocyte staining for flow cytometry was performed as previously described (16): integrin α_6 was detected by rat anti–mouse CD49f (Immunotech) and CD71 by biotinylated mouse anti–human CD71 (BD Biosciences — Pharmingen). Affinity-purified mAb HD-1 at 6 μg/ml was used to stain dermal cells for flow cytometry and in situ staining, detected with goat anti-mouse IgG–PE or anti-mouse IgG_1–FITC secondary antibodies (SouthernBiotech). Unconjugated isotype control antibodies were available in house (16) or purchased from SouthernBiotech. The following directly conjugated antibodies were used to phenotype dermal cell isolates: CD14-PE (IgG_{2a}; BD Biosciences — Pharmingen), CD31-PE (553373, IgG_{2a}; BD Biosciences — Pharmingen), CD33-FITC (IgG_1; eBioscience), CD68-FITC (IgG_1), HLA-DR–PE (IgG_{2b}), and CD45-FITC (IgG_1; eBioscience). vWF was detected with a rabbit polyclonal antibody (A0082; Dako). SMA was detected using antibody clone 1A4 (M0852; Dako) for cytospins and tissue sections. LAMA5 chain was detected using mAb 4C7 (GeneTex).

Dual staining for MSC markers and HD-1 was performed by using mAb HD-1 conjugated directly to FITC using a Zenon Fluorescein Mouse IgG_1 Kit (Invitrogen) and PE-labeled direct conjugates of antibodies against CD146/MCAM (R&D Systems), CD90 (clone 5E10; BD Biosciences — Pharmingen), CD73 (clone AD2; BD Biosciences — Pharmingen), and CD105 (clone SN6; Invitrogen). Immunostaining on sections of OCs for Ki67 was performed using clone MIB-1 (Dako) and cryosections of adult and neonatal skin for NG-2/CSPG-4 (Millipore) provided by Andy Möller (Peter MacCallum Cancer Centre).

Immunoprecipitation and blotting for α_1 integrin. P3 HFFs were lysed in IP-lysis buffer (1% NP40, 150 mM NaCl, 10 mM EDTA, 2.5 mM Tris-HCl, pH 7.5) supplemented with a protease inhibitor cocktail (Complete Mini Inhibitor Tablets, EDTA-free; Roche) for 30 minutes on ice and then 5 minutes at 97°C. The samples were spun at 16,100 *g* for 10 minutes at 4°C and the pellet discarded. The lysates were precleared by incubation with 50 μl DYNAL Dynabeads M-280 sheep anti-mouse IgG (washed in IP-lysis buffer) at 4°C for 16 hours on a rotating wheel. At the same time, 50-μl aliquots of Dynabeads were prearmed with either 1 ml neat HD-1 hybridoma supernatant or anti–α_1 integrin mAb TS2/7.1.1 (clone HB-245; ATCC), also by incubation at 4°C for 16 hours. The beads coupled to antibodies were then washed with IP-lysis buffer 4 times for use in IPs.

The protein lysates were placed on a magnet to separate the beads used for preclearing and the lysates transferred to tubes containing the antibody-armed beads (washed 4 times in lysis buffer to remove unbound antibody prior to use) and incubated at 4°C for 4 hours on a rotating wheel to precipitate proteins specifically recognized by the bound antibodies. All beads (including those used for preclearing) were washed 4 times with IP-lysis buffer and the bound proteins lysed in 3× Laemmli sample buffer (0.05 M Tris/HCl, pH 6.8, 25% glycerol, 3% SDS, bromphenol blue, water, and 150 μM DTT) at 97°C for 5 minutes. Samples were subjected to SDS-PAGE along with 6 μg purified $\alpha_1\beta_1$ integrin protein ($\alpha_1\beta_1$ integrin Triton X-100 formulation; catalog CC1015; Chemicon), antibody controls, and Novex Sharp prestained markers (Invitrogen) in pre-cast Novex 3-8% gradient Tris-Acetate (Invitrogen) gels. Proteins were then blotted onto a nitrocellulose membrane by means of the iBlot Dry Blotting System (Invitrogen). The nitrocellulose membrane was incubated in blocking buffer: 5% milk powder in Tris-buffered saline containing 0.001% Tween-20 (TBS-T) for 1 hour, washed with TBS-T, and then incubated for 1 hour with mouse anti–human integrin α_1 antibody (1:500; MAB1973, clone FB12; Chemicon). The membrane was washed 3 times for 10 minutes each in TBS-T and then incubated with goat anti-mouse HRP-conjugated antibody (1:5,000; Invitrogen). All incubations were performed at room temperature. After washing a further 3 times for 10 minutes with TBS-T, the membrane was incubated with HRP substrate (Amersham ECL Plus Western Blotting Detection System; GE Healthcare) for 2 minutes and x-ray films exposed for 5, 10, 30, and 60 seconds.

Submerged and organotypic cultures. Freshly sorted HD-1^{bri} cells were grown in α-MEM (GIBCO, Invitrogen) supplemented with 20% HyClone serum and 1 ng/ml PDGFβ; or in DMEM (GIBCO, Invitrogen) supplemented with 10% FBS (JRH Biosciences), both containing 200 mM L-glutamine, 500 mM pyruvate, 600 μg/ml penicillin/8 mg/ml gentamicin. OCs were established as described previously (43) with 2.5×10^4 P7 HFFs (or P0 HFFs) with or without 5,000 freshly isolated HD-1^{bri} cells in a type I collagen matrix (Organogenesis). Keratinocytes plated on the collagen gels were cultured submerged for 6 days, then raised to the air-liquid interface for another 14 days before harvest.

Microarray experiments. RNA was extracted from 15,000 sorted cells, using the QIAGEN RNeasy kit from 4 replicate independent sorts, each one composed by 4 pooled samples from different donors. The GeneChip Expression 3′ Amplification Two-Cycles Target Labeling kit (Affymetrix) and the Affymetrix Human Genome U133 Plus 2.0 arrays were used according to the manufacturer's protocol. The arrays were scanned in an Affymetrix GeneChip Scanner. The probe intensities were RMA normalized (44), and $\log_2$-transformed expression values for all probe sets compared between

samples using moderated *t* statistics (45) to quantify the relative differences between the samples. The resulting 2,288 differentially expressed probes were visualized using Eisen Cluster software and plotted using Treeview (http://jtreeview.sourceforge.net). Microarray data are available through the Gene Expression Omnibus database (accession number GSE17014; http://www.ncbi.nlm.nih.gov/geo/).

RT-PCR. Real-time PCR was performed with 10–20 ng of cDNA using SYBR Green (Applied Biosystems). Expression levels for LAMA5 were calculated using the comparative Ct method normalized to the GAPDH Ct value. Data were analyzed using the optical system from ABI Prism 7000 SDS software and Microsoft Excel 2000 to generate relative expression values.

The primer sequences used to detect the LAMA5 transcript by real-time PCR were as follows: forward primer sequence, 5′-TGGCTGGATTATGTACTCGTGG-3′, reverse primer sequence: 5′-CTGTAGCACCTACTTCGTGGCA-3′. GAPDH was used as a housekeeping control gene. The primer sequences for GAPDH were as follows: forward primer sequence, 5′-TCTGCTCCTCCTGTTCGACAGT-3′, reverse primer sequence, 5′-ACCAAATCCGTTGACTCCGAC-3′.

Immunoelectron microscopy for the LAMA5 chain. Fresh human neonatal foreskin tissue was collected immediately after circumcision, fixed in 4% PFA solution, cryoprotected in 2.3 M sucrose/0.1 M Sorensen's PBS, pH 7.4, and 4-μm cryosections were cut. Free aldehydes were blocked in 50 mM glycine PBS and nonspecific binding sites blocked in 3% goat serum in PBS with 0.05% Tween-20. Sections were labeled sequentially with mAb 4C7 against the α5 chain of laminin (GeneTex) or an isotype-matched negative IgG_{2a} control (mAb 1D4.5); FITC-conjugated secondary mAb; and finally Ultra Small Gold–conjugated mouse anti-FITC (12 μg/ml; Aurion). Sections were postfixed in 2% glutaraldehyde/0.8 M Sorensen's PBS, silver enhanced (R-Gent SE-LM; Aurion), postfixed in 2% osmium tetroxide, and infiltrated with Spurr's resin (ProSciTech). The pop-off technique was used to remove the sections from the glass slide. Ultrathin sections were cut using a diamond knife in the Reichert-Jung Ultracut E Ultramicrotome (Leica) and double stained with uranyl acetate and lead citrate. Samples were viewed and ultramicrographs taken with a Hitachi H-600 electron microscope.

Differentiation assays for pericytes. Fresh pericytes were obtained from human neonatal foreskin by FACS after staining with mAb HD-1 and collecting HD-1^{bri} cells, and cultured in α-MEM supplemented with 20% FCS and allowed to reach at least 80% confluency in 6-well plates. The medium was then replaced to induce differentiation as follows. For adipogenic assays, initial inductive medium made of DMEM supplemented with 10% v/v horse serum (GIBCO, Invitrogen) and final concentrations of 10^{-8} M hydrocortisone, 60 μM indomethacin (catalog I7378; Sigma-Aldrich), and 500 μM 1-isobutyl-3-methylxanthine (IBMX; catalog I5879; Sigma-Aldrich) was added for the first 4 days of the assay. After the inductive period, cells were re-fed with DMEM plus 10% horse serum for the remainder of the assay, typically 3 weeks, allowing for the accumulated presence of large cytoplasmic lipid vesicles. Cultures were stained for lipid by oil red O.

Osteogenic differentiation assays were performed on HD-1^{bri} sorted cells propagated in α-MEM 20% FCS that had reached 50%–70% confluency. The medium was replaced with α-MEM plus 20% FCS supplemented with final concentrations of 10^{-8} M dexamethasone, 100 μM ascorbate-2-phosphate, and 4 mM inorganic phosphate (KH_2PO_4) (Sigma-Aldrich and BDH) and changed every 3 days, and the cultures maintained for 2–4 weeks, allowing time for mineralization to occur. Cultures were stained for bone-derived calcium triphosphate mineral by von Kossa reagent.

Chondrogenic differentiation was induced by performing micromass pellet cultures. HD-1^{bri} sorted cells were expanded in α-MEM 20% FCS and then harvested, and 400,000–500,000 cells used to initiate the assay. Cells were washed and resuspended in PBS and centrifuged at a slower speed of 300 *g* to promote pellet formation and to remove all serum. The cells were then covered in 1 ml serum-deprived medium (10 ml of 10% [w/v] BSA/α-MEM, 1.0 ml recombinant human insulin [1 mg/ml stock], 1.0 ml transferrin [20 mg/ml stock], and 240 μl LDL to 88 ml of α-MEM) supplemented with 10 ng/ml TGF-β_3, 10 ng/ml BMP-6, and 50 ng/ml PDGF-BB (R&D Systems). Medium was replaced on the pellets every 3 days, and fresh growth factors were added with each medium change. Cultures were maintained for 3 weeks, and then the pellets were washed 2 times in PBS, fixed in formalin, and processed for embedding in paraffin. Pellets were sectioned at 3 μm, and slides were stained for matrix proteoglycans with Alcian blue and H&E.

Statistics. Quantitative and qualitative results from immunostaining, flow cytometry, OC experiments, and differentiation assays, were replicated in at least 3–5 independent experiments, and representative samples of these data were displayed only when reproducible results were obtained. For microarray experiments, the Benjamini and Hochberg multiple testing correction was used, and differentially expressed probe sets exhibiting greater than 2-fold change and an adjusted *P* value of less than 0.05 (i.e., 2,288 probes) were analyzed. Real-time PCR gene expression for *LAMA5* was analyzed using the 2-tailed Mann-Whitney *U* test to compare data from 3 independent sorting experiments and results considered statistically significantly different when *P* values of less than 0.05 were obtained.

Acknowledgments

We thank Ralph Rossi and Daud Dahur for their technical support in cell sorting. This work was supported by a National Health and Medical Research Council of Australia Project Grant 251535 and NIH grant R01 AR050013-01A2 to P. Kaur.

Received for publication January 12, 2009, and accepted in revised form June 17, 2009.

Address correspondence to: Pritinder Kaur, Epithelial Stem Cell Biology Lab, Peter MacCallum Cancer Centre, St Andrew's Place, East Melbourne, Victoria 3002, Australia. Phone: 61-3-9656-3714; Fax: 61-3-9656-1411; E-mail: pritinder.kaur@petermac.org.

1. Schofield, R. 1978. The relationship between the spleen colony-forming cell and the haemopoietic stem cell. *Blood Cells.* **4**:7–25.
2. Morrison, S.J., and Spradling, A.C. 2008. Stem cells and niches: mechanisms that promote stem cell maintenance throughout life. *Cell.* **132**:598–611.
3. Kobielak, K., Stokes, N., de la Cruz, J., Polak, L., and Fuchs, E. 2007. Loss of a quiescent niche but not follicle stem cells in the absence of bone morphogenetic protein signaling. *Proc. Natl. Acad. Sci. U. S. A.* **104**:10063–10068.
4. Moore, K.A., and Lemischka, I.R. 2006. Stem cells and their niches. *Science.* **311**:1880–1885.
5. Li, J., et al. 2003. Laminin-10 is crucial for hair morphogenesis. *EMBO J.* **22**:2400–2410.
6. Mueller, M.M., and Fusenig, N.E. 2004. Friends or foes—bipolar effects of the tumour stroma in cancer. *Nat. Rev. Cancer.* **4**:839–849.
7. Werner, S., Krieg, T., and Smola, H. 2007. Keratinocyte-fibroblast interactions in wound healing. *J. Invest. Dermatol.* **127**:998–1008.
8. Fusenig, N.E., et al. 1983. Growth and differentiation characteristics of transformed keratinocytes from mouse and human skin in vitro and in vivo. *J. Invest. Dermatol.* **81**:168s–175s.
9. Asselineau, D., Bernhard, B., Bailly, C., and Darmon, M. 1985. Epidermal morphogenesis and induction of the 67 kD keratin polypeptide by culture of human keratinocytes at the liquid-air interface. *Exp. Cell. Res.* **159**:536–539.
10. Rheinwald, J.G., and Green, H. 1975. Formation of a keratinizing epithelium in culture by a cloned cell line derived from a teratoma. *Cell.* **6**:317–330.
11. Zieske, J.D., et al. 1994. Basement membrane assembly and differentiation of cultured corneal cells: importance of culture environment and endothelial cell interaction. *Exp. Cell Res.* **214**:621–633.
12. Beppu, H., et al. 2008. Stromal inactivation of BMPRII leads to colorectal epithelial overgrowth and polyp formation. *Oncogene.* **27**:1063–1070.
13. Hirschi, K.K., and D'Amore, P.A. 1996. Pericytes in

the microvasculature. *Cardiovasc. Res.* **32**:687–698.
14. Crisan, M., et al. 2008. A perivascular origin for mesenchymal stem cells in multiple human organs. *Cell Stem Cell.* **3**:301–313.
15. Li, A., Pouliot, N., Redvers, R., and Kaur, P. 2004. Extensive tissue-regenerative capacity of neonatal human keratinocyte stem cells and their progeny. *J. Clin. Invest.* **113**:390–400.
16. Li, A., Simmons, P.J., and Kaur, P. 1998. Identification and isolation of candidate human keratinocyte stem cells based on cell surface phenotype. *Proc. Natl. Acad. Sci. U. S. A.* **95**:3902–3907.
17. Shepro, D., and Morel, N.M. 1993. Pericyte physiology. *FASEB J.* **7**:1031–1038.
18. Armulik, A., Abramsson, A., and Betsholtz, C. 2005. Endothelial/pericyte interactions. *Circ. Res.* **97**:512–523.
19. Gitlin, J.D., and D'Amore, P.A. 1983. Culture of retinal capillary cells using selective growth media. *Microvasc. Res.* **26**:74–80.
20. Kaur, P., and Li, A. 2000. Adhesive properties of human basal epidermal cells: an analysis of keratinocyte stem cells, transit amplifying cells, and postmitotic differentiating cells. *J. Invest. Dermatol.* **114**:413–420.
21. Szabowski, A., et al. 2000. c-Jun and JunB antagonistically control cytokine-regulated mesenchymal-epidermal interaction in skin. *Cell.* **103**:745–755.
22. Miki, T., et al. 1991. Expression cDNA cloning of the KGF receptor by creation of a transforming autocrine loop. *Science.* **251**:72–75.
23. Marchese, C., et al. 2001. Fibroblast growth factor 10 induces proliferation and differentiation of human primary cultured keratinocytes. *J. Invest. Dermatol.* **116**:623–628.
24. Blanton, R.A., Kupper, T.S., McDougall, J.K., and Dower, S. 1989. Regulation of interleukin 1 and its receptor in human keratinocytes. *Proc. Natl. Acad. Sci. U. S. A.* **86**:1273–1277.
25. Smola, H., Thiekotter, G., and Fusenig, N.E. 1993. Mutual induction of growth factor gene expression by epidermal-dermal cell interaction. *J. Cell Biol.* **122**:417–429.
26. Maas-Szabowski, N., Stark, H.J., and Fusenig, N.E. 2000. Keratinocyte growth regulation in defined organotypic cultures through IL-1-induced keratinocyte growth factor expression in resting fibroblasts. *J. Invest. Dermatol.* **114**:1075–1084.
27. El Ghalbzouri, A., Jonkman, M.F., Dijkman, R., and Ponec, M. 2005. Basement membrane reconstruction in human skin equivalents is regulated by fibroblasts and/or exogenously activated keratinocytes. *J. Invest. Dermatol.* **124**:79–86.
28. Pouliot, N., Redvers, R.P., Ellis, S., Saunders, N.A., and Kaur, P. 2005. Optimization of a transplant model to assess skin reconstitution from stem cell-enriched primary human keratinocyte populations. *Exp. Dermatol.* **14**:60–69.
29. Legg, J., Jensen, U.B., Broad, S., Leigh, I., and Watt, F.M. 2003. Role of melanoma chondroitin sulphate proteoglycan in patterning stem cells in human interfollicular epidermis. *Development.* **130**:6049–6063.
30. Belkin, V.M., Belkin, A.M., and Koteliansky, V.E. 1990. Human smooth muscle VLA-1 integrin: purification, substrate specificity, localization in aorta, and expression during development. *J. Cell Biol.* **111**:2159–2170.
31. Lissitzky, J.C., et al. 2000. Endoproteolytic processing of integrin pro-alpha subunits involves the redundant function of furin and proprotein convertase (PC) 5A, but not paired basic amino acid converting enzyme (PACE) 4, PC5B or PC7. *Biochem. J.* **346**:133–138.
32. Hemler, M.E., Jacobson, J.G., and Strominger, J.L. 1985. Biochemical characterization of VLA-1 and VLA-2. Cell surface heterodimers on activated T cells. *J. Biol. Chem.* **260**:15246–15252.
33. Bergers, G., Song, S., Meyer-Morse, N., Bergsland, E., and Hanahan, D. 2003. Benefits of targeting both pericytes and endothelial cells in the tumor vasculature with kinase inhibitors. *J. Clin. Invest.* **111**:1287–1295.
34. Caplan, A.I. 2008. All MSCs are pericytes? *Cell Stem Cell.* **3**:229–230.
35. Pouliot, N., Saunders, N.A., and Kaur, P. 2002. Laminin 10/11: an alternative adhesive ligand for epidermal keratinocytes with a functional role in promoting proliferation and migration. *Exp. Dermatol.* **11**:387–397.
36. Kishimoto, T., et al. 1999. *Leukocyte typing VI.* Garland Publishing, Inc. New York, New York, USA. 1376 pp.
37. Beger, B., Robertson, K., Evans, A., Grant, A., and Berg, J. 2006. Expression of endoglin and the activin receptor-like kinase 1 in skin suggests a role for these receptors in normal skin function and skin tumorigenesis. *Br. J. Dermatol.* **154**:379–382.
38. Quintanilla, M., et al. 2003. Expression of the TGF-beta coreceptor endoglin in epidermal keratinocytes and its dual role in multistage mouse skin carcinogenesis. *Oncogene.* **22**:5976–5985.
39. Lorenz, K., et al. 2008. Multilineage differentiation potential of human dermal skin-derived fibroblasts. *Exp. Dermatol.***17**:925–932.
40. Toma, J.G., et al. 2001. Isolation of multipotent adult stem cells from the dermis of mammalian skin. *Nat. Cell Biol.* **3**:778–784.
41. Toma, J.G., McKenzie, I.A., Bagli, D., and Miller, F.D. 2005. Isolation and characterization of multipotent skin-derived precursors from human skin. *Stem Cells.* **23**:727–737.
42. Jahoda, C.A., Whitehouse, J., Reynolds, A.J., and Hole, N. 2003. Hair follicle dermal cells differentiate into adipogenic and osteogenic lineages. *Exp. Dermatol.* **12**:849–859.
43. Gangatirkar, P., Paquet-Fifield, S., Li, A., Rossi, R., and Kaur, P. 2007. Establishment of 3D organotypic cultures using human neonatal epidermal cells. *Nature Protocols.* **2**:178–186.
44. Irizarry, R.A., et al. 2003. Summaries of Affymetrix GeneChip probe level data. *Nucleic Acids Res.* **31**:e15.
45. Bengtsson, H., Irizarry, R., Carvalho, B., and Speed, T.P. 2008. Estimation and assessment of raw copy numbers at the single locus level. *Bioinformatics.* **24**:759–767.